VORTEX EVOLUTION NEAR A SOLID WALL UNDER THE INFLUENCE OF A POTENTIAL WAVE

K.M. KULIK, A.V. TUR[1], V.V. YANOVSKY

Institute for Single Crystals, Nat. Acad. Sci. of Ukraine
(60, Lenin Avenue, Kharkiv 61001, Ukraine; e-mail: yanovsky@isc.kharkov.ua),

[1]**Center D'etude Spatiale Des Rayonnements, C.N.R.S.-U.P.S.**
(Avenue Colonel-Roche, 9, TOULOUSE CEDEX 4)

UDC 532

The influence of potential oscillation modes on the motion of a point vortex near a solid wall is studied. The equations that describe the motion of a point vortex in the given field of a potential wave near the solid wall are derived. It is shown that the character of the vortex motion changes dramatically under the influence of a potential wave, and the possible modes of the vortex motion are analyzed.

1. Introduction

In all fluid media, there are important objects of the two types. These are waves and vortices. The role of linear waves is significant and well studied. From the physical point of view, those waves can be considered as distinctive universal particles. The approach based on the properties of these particles and their interaction facilitates the understanding of many linear and nonlinear phenomena. In a certain sense, vortices can also be considered as quasi-particles. These particles are also useful to understand many phenomena in fluid media. The difficulty lies in the fact that vortices are the solutions of nonlinear equations of fluid dynamics. The linear approximation is of no use for vortices. This explains the difficulties encountered in studying vortices. The study of vortices is further complicated by the fact that the reduction of the problem to a one-dimensional one, which is a fruitful approach for nonlinear waves, is not applicable to vortices. Vortices are always multidimensional. Most studied are the vortices in the two-dimensional ideal fluid dynamics. These are the point vortices, which resemble quasi-particles [1]. The equations of the vortex motion in the Hamilton form have been derived by Kirchhoff [2]. The evolution of interacting point vortices is quite well understood. The motion of two vortices was studied in early works [1] and [2] (see, for example, [3]). The evolution of three vortices was analyzed in detail in works [4, 5] (see also [6, 7]). In the case of arbitrary positions and the appearance of a chaotic motion, the problem of four and more vortices was proved in works [8–11] to be non-integrable. The study of the influence of a fluid boundary on the motion of vortices was started by Helmholtz. He considered the motion of one point vortex in the ideal fluid bounded by a plane. The modern theory of the vortex motion in an arbitrary region was founded in work [12] (see, for example, [13]). In other words, the properties of waves and point vortices separately are well studied at the present time. However, vortices and waves in the fluid systems are observed simultaneously, as a rule. Therefore, it is very important to study the influence of these two hydrodynamical objects on each other. The basis of the study of this influence was founded by Lighthill [14, 15]. He studied the generation of potential waves by the vortex motion. The study of the inverse influence of potential waves on the vortex evolution was started quite recently [16, 17]. It was found that the character of the evolution of point vortices changes dramatically under the influence of potential waves. One of the examples is the collapse of vortices (of the same sign of vorticity) under the influence of potential oscillations with even a small amplitude [16, 17]. In the absence of potential oscillations, the collapse of point vortices with vorticities of the same sign is impossible.

In the present work, we consider the influence of potential vibrational modes on the point vortex motion near the solid wall. It is shown that the character of vortex motion changes qualitatively. All possible modes of the vortex motion under the action of a potential wave are analyzed.

From the physical point of view, the simplest influence on the vortex motion is realized by a potential wave propagating along the wall. In this case, the wave influence is reduced to the nonlinear oscillations of the longitudinal component of the vortex velocity with the frequency different from the wave frequency. The distance of the vortex to the wall remains constant, as in the absence of the potential wave. This is the case of an exactly integrable problem, and its explicit solutions are presented in this paper. A more complicated influence is rendered by the wave obliquely incident on the wall. In this case, the vortex can approach the wall and move away from the wall under the influence of the incident and reflected waves. In the present work, we analyze all the types of nonlinear different modes as functions of the wave and vortex parameters. The existence of a variety of modes creates the possibility of a non-trivial control over the vortex by means of potential waves. The obtained results can be used in a number of physical applications. For example, using the laws of vortex motion in the wave field, we can reconstruct the total field of fluid velocity and study a transfer of a passive admixture near the wall. This transfer is important in a number of applications. Another important example is the formation of vortex structures during the line vortex motion near the wall. It follows from the results obtained in this work that, under the influence of localized potential packets, a line vortex can develop local deformations which will lead to the creation of localized vortex structures. In particular, under small horseshoe-shaped deformations of the vortex line, we can observe the solitons propagating along the line vortex. The larger the deformations, the more complicated are the vortex structures. In this case, the dissipative processes will lead to the transformation and formation of localized vortex structures not related to the initial line vortex. Here, we observe a specific mechanism of the vorticity increasing near the wall. The obtained results explain the mechanism and the initial stage of the formation of vortex structures.

2. Equations of Vortex Motion in a Potential Wave Field near the Wall

First, consider the velocity field of a potential wave in the compressible fluid in the presence of a solid wall. The amplitudes of potential waves are assumed to be small. In this case, we obtain a potential mode in the compressible fluid in the form of sound waves (see, for example, [18]). In the presence of a wall, we observe two most interesting steady-state cases of the potential wave propagation. These are the propagation of a wave along the wall and the oblique incidence of a wave onto the boundary. Let the fluid be located in the half space $y > 0$, and let the impenetrable boundary be placed at $y = 0$. Consider, without any loss of generality, potential waves propagating in the (x, y) plane.

In the first case, the velocity field potential of a sound wave takes the form

$$\varphi_{1s} = a_0 \cos(k_x x - \Omega t). \tag{1}$$

Here, a_0 is the initial value of the wave amplitude, $\vec{k} = (k_x, 0)$ is the wave vector, and $\Omega = ck_x$ is the frequency (c is the sound velocity in the medium). In the second case, the velocity field potential is determined by both the incident wave and the wave reflected from the solid boundary at $y = 0$:

$$\varphi_{2s} = a_0 \cos(yk_y) \cos(k_x x - \Omega t). \tag{2}$$

In this case, the angle of incidence α of the wave on the boundary is determined from the relation $\tan(\alpha) = k_y/k_x$, and $\Omega = ck$.

Now we consider the equations of motion of a point vortex near the boundary under the influence of a given potential wave. In the derivation of these equations, we use the approach developed in works [16, 17]. It is well known that the vortex is frozen into the fluid, and hence the vortex velocity is the same as the fluid velocity (V_x, V_y) at the point of the vortex location. This means that

$$\frac{dx_1}{dt} = V_x|_{x=x_1 y=y_1},$$

$$\frac{dy_1}{dt} = V_y|_{x=x_1 y=y_1},$$

where (x_1, y_1) is the position of the vortex in the half-plane $y > 0$. According to the Helmholtz theorem [19], the velocity field can be decomposed into the sum of the vortical and potential components, $\vec{V} = \vec{v}_v + \vec{v}_p$. The potential component is determined by the given external flux and the waves induced by the vortex motion. However, the contributions from the induced potential waves are proportional to the square of the Mach number (see [14]), and these can be neglected in the main approximation [16, 17].

The vortical velocity field of a single vortex near the solid wall is well known [13], $\vec{v}_v = (\Gamma/4\pi y, 0)$, and the potential components of the velocity are $\vec{v}_p = \nabla\varphi$ (the potentials are given above). The equations of the vortex motion in the field of the given incident and reflected sound waves (2) can be written in the form

$$\frac{dX}{d\tau} = \frac{\delta}{Y} - 1 - \varepsilon \cos Y \sin X, \tag{3}$$

$$\frac{dY}{d\tau} = \Delta \sin Y \cos X, \tag{4}$$

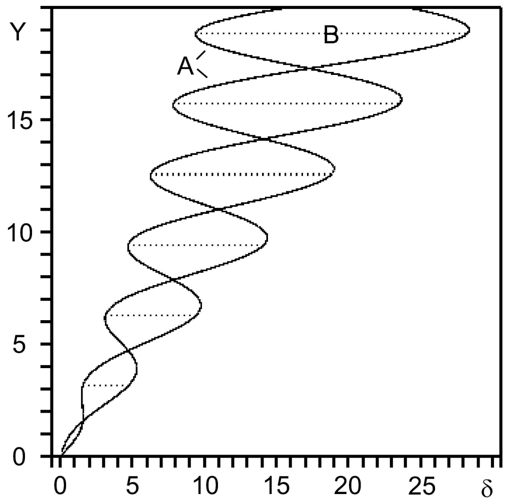

Fig. 1. Positions of the stationary points A and B on the x axis for various values δ and a fixed $\varepsilon = 0.5$. The solid lines correspond to stationary points of type A, and the dashed lines correspond to stationary points of type B. One dashed line corresponds to two points of type B, because they have the same y coordinates but different x coordinates. It can be seen that the change in the number of the stationary points with increase in δ is related to the generation and annihilation of the stationary points

where we have introduced the dimensionless variables $\tau = \Omega t$, $Y = yk_y$ and have made a transition into the moving coordinate system $X = k_x x - \tau$. Here, we obtain the dimensionless parameters $\varepsilon = \frac{a_0 k_x^2}{\Omega}$, $\Delta = \frac{a_0 k_y^2}{\Omega}$, and $\delta = \frac{\Gamma k_x k_y}{4\pi c k}$ that characterize the amplitudes of the velocity components and the vortex intensity, respectively.

For a sound wave propagating along the boundary (1), the equation of the vortex motion takes the form

$$\frac{dX}{d\tau} = \frac{\sigma}{Y} - \varepsilon \sin X - 1, \tag{5}$$

$$\frac{dY}{d\tau} = 0. \tag{6}$$

Here, the parameter $\sigma = \frac{\Gamma k_x}{4\pi c}$ characterizes the vortex intensity. In the absence of potential vibrations, these systems of equations are reduced to the known equations of the vortex motion near a solid wall (see, for example, [13]). In this case, the character of the vortex motion is very simple. A vortex moves along the wall keeping the same distance from the wall at the constant velocity $V_v = \Gamma/4\pi y_0$ that depends on the vorticity Γ and the initial distance y_0 from the wall.

Using the obtained equations, we will analyze the possible modes of the vortex motion under the action of a potential wave near the solid wall.

3. Vortex Motion in the Field of the Incident and Reflected Sound Waves

Here, we analyze qualitatively the system of equations (3) and (4). The coordinates of the stationary points are determined by zeros of the right-hand sides of these equations. Namely,

$$\frac{\delta}{Y} - 1 - \varepsilon \cos Y \sin X = 0, \tag{7}$$

$$\Delta \sin Y \cos X = 0. \tag{8}$$

Equation (8) has two types of solutions, and hence there appear two sets of stationary points. Denote the coordinates of these points by subscripts A and B. The stationary points create a periodic system of points along the x axis with period 2π. This means that the phase portraits of the system of equations (3), (4) are periodic along the x axis with period 2π.

In case A, the x coordinates of stationary points obey the equation

$$X_A^* = \frac{\pi}{2} \pm k\pi, \tag{9}$$

where $k = 0, 1, 2, \ldots$.

From Eq. (8), we obtain the y coordinates of the stationary points B as

$$Y_B^* = \pm n\pi, \tag{10}$$

where $n = 1, 2, \ldots$. Naturally, only the stationary points located in the region occupied by a fluid, with $y > 0$, have a physical sense. Therefore in case B, we consider only $Y_B^* = n\pi$. The positions of the stationary points A on the y axis are determined by the equation

$$\frac{\delta}{Y_A^*} = 1 - \alpha_k \varepsilon \cos(Y_A^*), \tag{11}$$

where $\alpha_k = \sin(\frac{\pi}{2} \pm k\pi) = (-1)^k$. The number of solutions of this equation and, hence, the number of stationary points A in one period depend significantly on the parameters ε and δ. Figure 1 shows how the number of stationary points A changes with the change in the parameter δ at the fixed parameter ε. Figure 1 can be considered, in fact, as a bifurcation diagram with respect

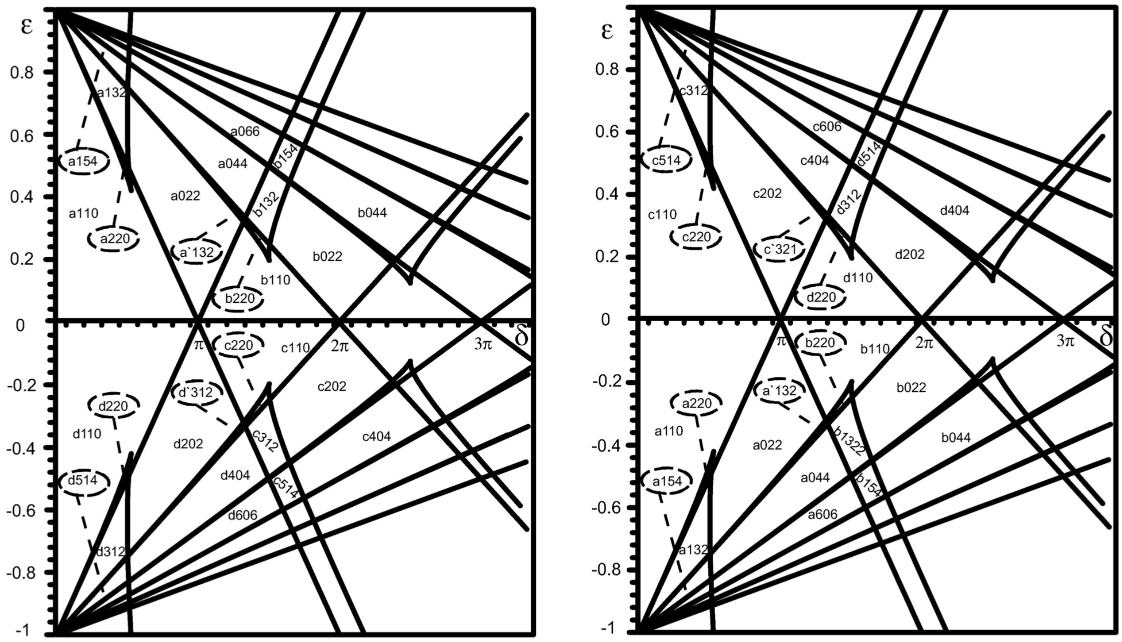

Fig. 2. Regions of the parameters (ε, δ) that determine the number and type of stationary points in the phase portraits. The left and right graphs show, respectively, the regions of parameters for $\Delta > 0$ and $\Delta < 0$. The first digit in the region number denotes the number of stationary points of type A of the hyperbolic type, the second digit corresponds to the number of elliptic stationary points of type A, and the third digit means the number of hyperbolic stationary points of type B for the numbers starting from a and b or the number of nodes for the numbers starting from c and d. The phase portraits with the same digits but different letters differ from one another by the shift along the x axis by a half-period π. Thus, $a \longleftrightarrow b$ $c \longleftrightarrow d$ at the shift by π

to the parameter δ. The bifurcations related to a change in the number of stationary points correspond to the birth and annihilation of the pairs of stationary points A and B. Analyzing Eq. (11), we can find the regions with different numbers of stationary points of type A in the plane of parameters.

Analogously, the equation that determines the positions of stationary points B and their numbers takes the form

$$\sin(X_B^*) = \frac{\delta - \pi n}{\pi n \varepsilon}\alpha_n, \quad (12)$$

where $\alpha_n = \cos(n\pi)$. At a fixed n, this equation has solutions if the inequality

$$\left|1 - \frac{\delta}{n\pi}\right| \leq |\varepsilon|$$

is fulfilled. These conditions determine, at various values of n, the regions in the parameter plane with different numbers of stationary points B in one period of the phase portrait. The positions of stationary points B on the y axis at various values δ and a fixed ε are also shown in Fig. 1.

Now we consider the types of stationary points. The characteristic equation for stationary points (X_A^*, Y_A^*) takes the form

$$\lambda_A^2 = \alpha_k \Delta \sin(Y_A^*)\left(\frac{\delta}{Y_A^{*2}} - \alpha_k \varepsilon \sin(Y_A^*)\right).$$

It can be easily seen that the stationary points A can be only elliptic (if the condition $\alpha_k \Delta \sin(Y_A^*)\left(\frac{\delta}{Y_A^{*2}} - \alpha_k \varepsilon \sin(Y_A^*)\right) < 0$ is satisfied) or hyperbolic (if $\alpha_k \Delta \sin(Y_A^*)\left(\frac{\delta}{Y_A^{*2}} - \alpha_k \varepsilon \sin(Y_A^*)\right) > 0$). The parameter Δ enters these conditions in a trivial manner, and hence their validity depends only on its sign. When the sign of Δ changes, the hyperbolic stationary points change to elliptic, and the elliptic points change to hyperbolic, without change in their position in the phase space.

Analogously, the type of points B is determined by the characteristic equation

$$\lambda^2 - \alpha_n \lambda \cos(X_B^*)(\Delta - \varepsilon) - \Delta\varepsilon \cos^2(X_B^*) = 0.$$

This equation has solutions of the form

$$\lambda_B^{\pm} = \frac{\cos(X_B^*)}{2}[\alpha_n(\Delta - \varepsilon) \pm (\Delta + \varepsilon)].$$

This implies that, at $\Delta > 0, \varepsilon > 0$ or $\Delta < 0, \varepsilon < 0$, the points are of hyperbolic type, and, at $\Delta < 0, \varepsilon > 0$ or $\Delta > 0, \varepsilon < 0$, the stationary points are stable or unstable nodes. In this case, the influence of the parameter Δ is more essential. Summarizing the data on the number of stationary points in one period and on their types, we can construct the regions of parameters for all possible types of the phase portraits realized in a given mode (Fig. 2). The total region of parameters is divided into the infinite number of regions with various types of phase portraits. Some of these regions with relatively simple phase portraits are shown in Fig. 2. The choice of regions is dictated by physical restrictions such as $|\varepsilon| \leq 1$ and by the condition that δ is not very big (for example, $|1 - \delta/4\pi| \leq \varepsilon$). The construction of the rest regions and their geometrical positions can be easily extended on the whole plane of parameters. The numbering scheme is chosen in accordance with the number and type of stationary points on the phase portrait at the given values of parameters.

Now we consider the motion modes of vortices in the moving coordinate frame. It is clear that the complexity of the phase portraits and the modes of vortex motions increases with the number of stationary points in one period. The general feature is the division of the phase space into separate cells by separatrices. The number of these cells increases with the number of stationary points in one period. In each cell, only three types of behavior can be realized. These are the nonlinear oscillations of captured vortices with zero average velocity along the x axis, the nonlinear oscillations of flying vortices with non-zero average velocity along the x axis, and, finally, the oscillations with the non-linear relaxation into a stable node inside the cell. This last type of behavior is unusual. During the relaxation, the memory about the initial state of the vortex is completely lost. Such a behavior is typical of dissipative systems. Figure 3 shows the simple examples of the phase portraits characteristic of various regions of parameters.

The phase portraits on the left part of Fig. 3 are plotted for $\Delta > 0$, $\varepsilon > 0$ and $\Delta < 0$, $\varepsilon < 0$, and those on the right part are constructed for $\Delta < 0$, $\varepsilon > 0$ and $\Delta > 0$, $\varepsilon < 0$. These portraits exhibit a certain symmetry. It is easy to see that these portraits transit into one another at the permutation of elliptic stationary points with hyperbolic points and vice versa. Let us start with the analysis of the phase portraits shown in Fig. 3 on the left. It can be seen that the phase portraits are periodic along the x axis with period 2π. These portraits consist of the cells bounded by the separatrices of hyperbolic stationary points. Inside these cells, there are elliptic stationary points. A vortex, whose initial coordinates fall in such a cell, becomes captured and begins to nonlinearly oscillate in the longitudinal and transverse directions near the elliptic point. If the initial position of the vortex is below or above the cell, the vortex moves along the boundary by oscillating nonlinearly in the transverse direction.

The phase portraits shown on the right in Fig. 3 also consist of cells. Two upper phase portraits on the right have the cells similar to those in the phase portraits on the left. Hence, there is a similarity in the modes of the vortex motion. In two bottom phase portraits on the right, there appear the cells of a different type. The vertices of these cells are occupied by the hyperbolic stationary points, and there are one stable and one unstable nodes on the two separatrices joining the vertices. These regions are clearly visible in the bottom right phase portrait. The appearance of nodes means that the vortex with initial conditions belonging to the corresponding cell will be inevitably attracted to a stable node. Thus, we observe one more mode of the vortex motion, when it is captured by a stable node. Then the vortex velocity becomes equal to zero (in the moving coordinate system).

In the conclusion of this section, we discuss the region of parameters, in which the integrability of the equations of the vortex motion can be easily proved. The system of equations (3), (4) can be reduced to the quasi-Hamilton form

$$\Delta \frac{dX}{dt} = \frac{\partial H}{\partial Y}, \tag{13}$$

$$\varepsilon \frac{dY}{dt} = -\frac{\partial H}{\partial X}. \tag{14}$$

The role of the Hamiltonian H is played by the function

$$H = \Delta\delta \ln Y - \Delta Y - \varepsilon\Delta \sin Y \sin X.$$

If we set $\Delta = \varepsilon$, the system of equations (13),(14) becomes a Hamilton system with the time-independent Hamiltonian. Thus, according to the Liouville theorem on the integrability of Hamilton systems, this system is integrable in quadratures [21]. We note that if the condition $\varepsilon = \Delta$ is set in the parameter plane (ε, δ), the integrable systems belong to the regions ($\varepsilon > 0$, $\delta > 0$, $\Delta > 0$) and ($\varepsilon < 0$, $\delta > 0$, $\Delta < 0$). In the general case, the initial system of equations cannot be reduced to the Hamilton system. This can be understood taking into account the existence of the modes with node-type stationary points, which cannot appear in the Hamilton systems.

 ISSN 0503-1265. Ukr. J. Phys. 2006. V. 51, N 10

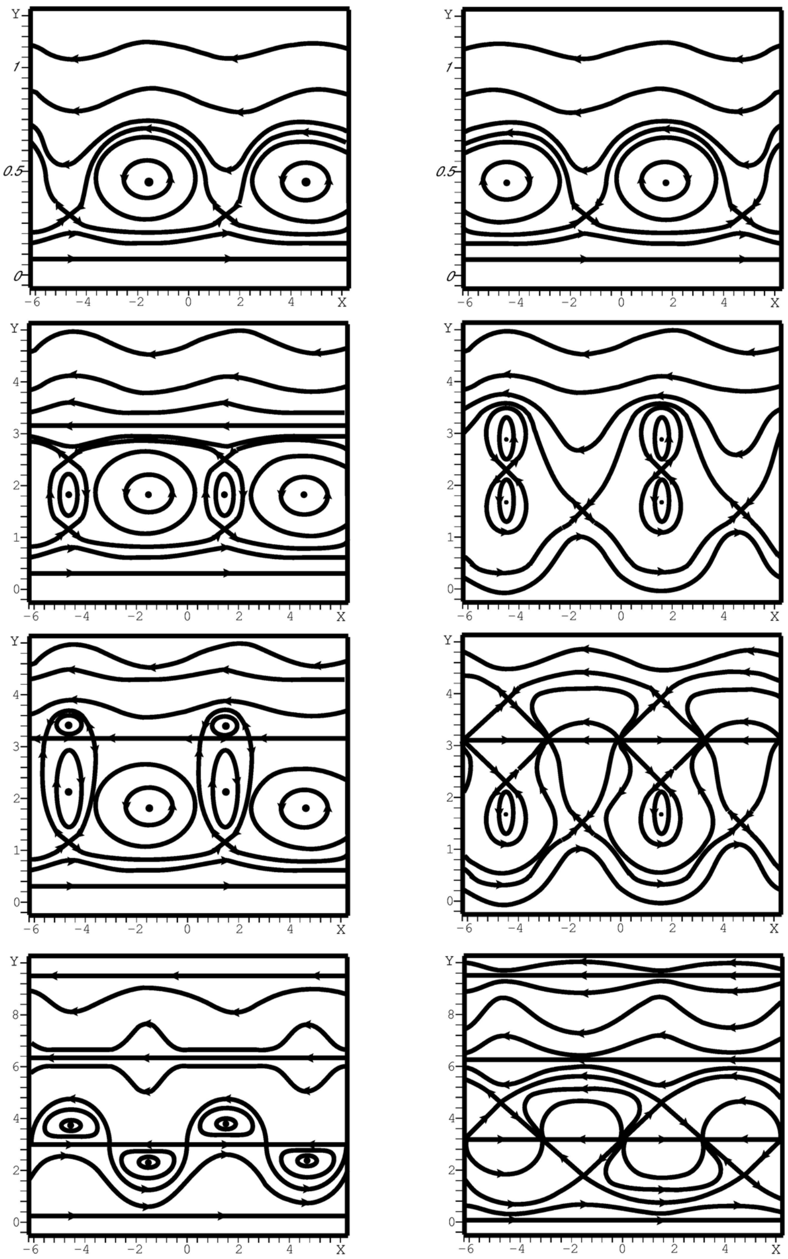

Fig. 3. On the left (from top to bottom) the typical phase portraits are shown for the parameters belonging to the regions: $a110$ ($\delta = 1$, $\varepsilon = 0.4$, $\Delta = 0.5$), $a220$ ($\delta = 1.5$, $\varepsilon = 0.5$, $\Delta = 0.5$), $a132$ ($\delta = 1.2$, $\varepsilon = 0.7$, $\Delta = 0.5$), $a022$ ($\delta = 3$, $\varepsilon = 0.4$, $\Delta = 0.5$). On the right: $c110$ ($\delta = 3$, $\varepsilon = 0.4$, $\Delta = -0.5$), $c220$ ($\delta = 4$, $\varepsilon = 0.5$, $\Delta = -0.5$), $c312$ ($\delta = 1.2$, $\varepsilon = 0.7$, $\Delta = -0.5$), $c202$ ($\delta = 3$, $\varepsilon = 0.4$, $\Delta = -0.5$)

4. Vortex Evolution under the Influence of a Sound Wave Propagating along the Fluid Boundary

Consider now the vortex behavior under the influence of a sound wave. From the system of equations (5), (6), we obtain the conservation of the distance between the vortex and the wall, $y(\tau) = y_0$. This means, in fact, that the vortex motion is one-dimensional. In other words, the phase space (x, y) is stratified in one-dimensional layers parallel to the wall. The dynamics of the vortex in each layer is determined by the presence or absence of the stationary points in this layer. This is an exactly integrable problem. The form of the solution depends on

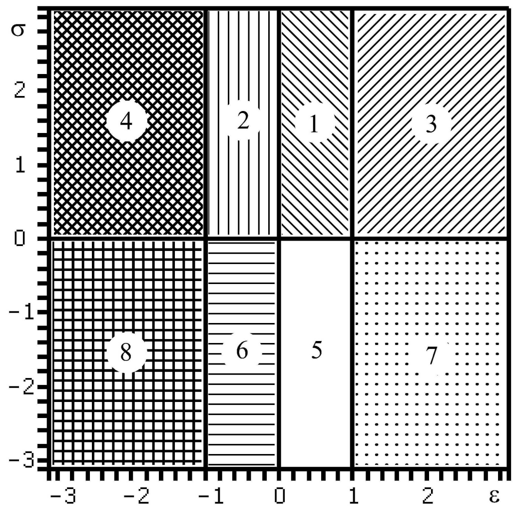

Fig. 4. Various dashed patterns show the regions in the (σ, ε) plane, in which the phase portraits differ qualitatively in the physically allowed region $y > 0$

the relation between the parameters of the system and the distance of the layer from the wall. For example, at $(\frac{\sigma}{y_0} - 1)^2 > \varepsilon^2$, the solution looks as

$$x(\tau) = \frac{1}{2}\arctan\left[\tan\left(\frac{\tau\sqrt{(\frac{\sigma}{y_0}-1)^2-\varepsilon^2}}{2} + \right.\right.$$

$$\left.+\arctan\left(\frac{(\frac{\sigma}{y_0}-1)\tan(\frac{x_0}{2})-\varepsilon}{\sqrt{(\frac{\sigma}{y_0}-1)^2-\varepsilon^2}}\right)\right)\times$$

$$\left.\times\,\frac{\sqrt{(\frac{\sigma}{y_0}-1)^2-\varepsilon^2}+\varepsilon}{(\frac{\sigma}{y_0}-1)}\right]. \tag{15}$$

At $(\frac{\sigma}{y_0} - 1)^2 < \varepsilon^2$, we get

$$x(\tau) = \frac{1}{2}\arctan\left[\frac{\varepsilon + \sqrt{\varepsilon^2 - (\frac{\sigma}{y_0}-1)^2}}{1 - e^{\tau\sqrt{\varepsilon^2-(\frac{\sigma}{y_0}-1)^2}}g} + \right.$$

$$\left.+\frac{\left[-\varepsilon + \sqrt{\varepsilon^2 - (\frac{\sigma}{y_0}-1)^2}\right]e^{\tau\sqrt{\varepsilon^2-(\frac{\sigma}{y_0}-1)^2}}g}{1 - e^{\tau\sqrt{\varepsilon^2-(\frac{\sigma}{y_0}-1)^2}}g}\right], \tag{16}$$

where

$$g \equiv \left|\frac{(\frac{\sigma}{y_0}-1)\tan(\frac{x_0}{2}) - \varepsilon - \sqrt{\varepsilon^2 - (\frac{\sigma}{y_0}-1)^2}}{(\frac{\sigma}{y_0}-1)\tan(\frac{x_0}{2}) - \varepsilon + \sqrt{\varepsilon^2 - (\frac{\sigma}{y_0}-1)^2}}\right|.$$

The analysis of these solutions is quite complicated. It is simpler to analyze the phase portraits and thus to establish all possible qualitative modes of the vortex motion.

Positions of the stationary points x^* in the one-dimensional layer parametrized by the initial value y_0 are determined by the equation

$$\frac{\sigma}{y_0} - \varepsilon\sin x^* - 1 = 0. \tag{17}$$

This equation has solutions if the inequality

$$\left|\frac{\sigma}{y_0} - 1\right| \leq |\varepsilon|$$

is satisfied and if the stationary points lie periodically in the layers $y = y_0$. This means that they are present in the modes, for which the exact solution takes the form (16). The type of a stationary point in the layer is determined by the characteristic equation

$$\lambda = -\varepsilon\cos x^*.$$

If $\lambda < 0$, the stationary point is a stable node. But if $\lambda > 0$, the stationary point is an unstable node.

Thus, the phase plane is stratified into one-dimensional layers $y = y_0$, in which the stationary points are located. Stationary points that belong to different layers lie in the phase space on the curves determined by the function

$$y = \frac{\sigma}{1 + \varepsilon\sin(x^*)}.$$

It can be seen that there are eight types of the phase portraits depending on the parameters σ, ε. In the (σ, ε) parameter plane, these regions are determined by the inequalities *1* — $(\sigma > 0, 0 < \varepsilon < 1)$, *2* — $(\sigma > 0, -1 < \varepsilon < 0)$, *3* — $(\sigma > 0, 1 < \varepsilon)$, *4* — $(\sigma > 0, \varepsilon < -1)$, *5* — $(\sigma < 0,\ 0 < \varepsilon < 1)$, *6* — $(\sigma < 0, -1 < \varepsilon < 0)$, *7* — $(\sigma < 0, 1 < \varepsilon)$, *8* — $(\sigma < 0, \varepsilon < -1)$ (see Fig. 4).

The typical phase portraits for each region are shown in Fig. 5. The phase portraits for the parameter regions *5, 6* are not shown, as they do not contain layers with stationary points.

The dynamics of a vortex in the layers containing the stationary points is reduced to the vortex relaxation to the stable node and hence to the zero vortex velocity in the moving coordinate frame. It should be pointed out that there occurs a partial loss of the memory of the initial vortex position in the corresponding layer. In layers without the stationary points, the vortex velocity is determined by solution (15) and has a periodic

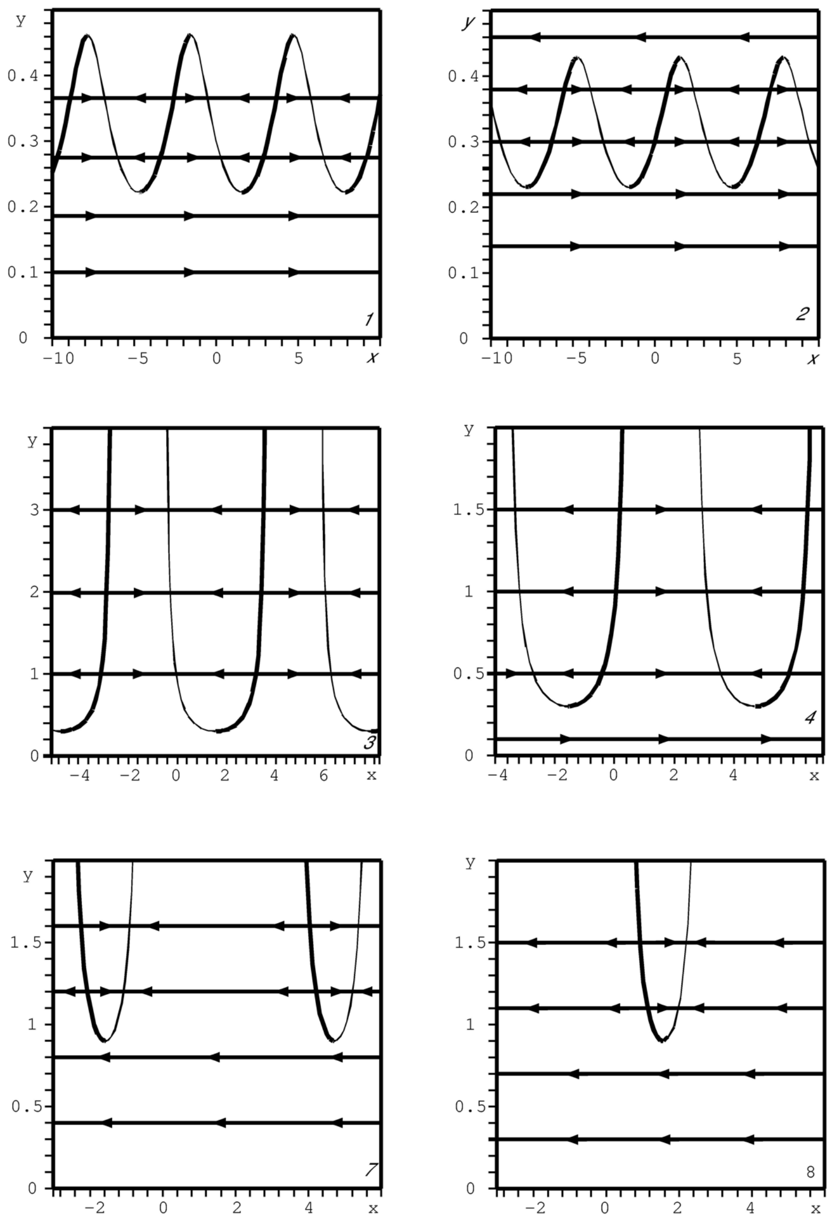

Fig. 5. Typical phase portraits for various parameter regions. The number of the corresponding parameter region (see Fig. 4) is shown in the right bottom corner of each phase portrait. The bold line shows the positions of unstable nodes, and the thin line shows the positions of stable nodes

longitudinal component $-\varepsilon \sin x(\tau)$ against the background of the constant component $\frac{\sigma}{y_0} - 1$. The oscillating velocity component has discontinuities (see Fig. 6), and its oscillation period $T = \pi/(2\sqrt{(\frac{\sigma}{y_0} - 1)^2 - \varepsilon^2})$ depends on the parameters σ, ε and the distance from the wall. In the parameter regions *1* and *2*, these modes are realized near the wall and far away from the wall ($y_0 < y_{c1} = \sigma/(1-|\varepsilon|)$ and $y_0 > y_{c2} = \sigma/(1+|\varepsilon|)$). In the parameter regions *3,4,7,* and *8*, such modes are possible only near the wall. In the regions *5* and *6*, only such modes are realized.

5. Conclusion

In conclusion, we discuss the main qualitative changes in the vortex evolution under the influence of a potential

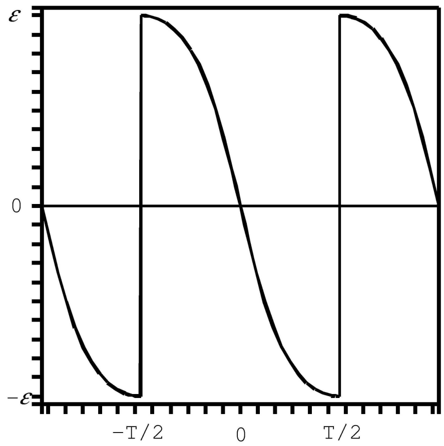

Fig. 6. Typical shape of the oscillating component of the velocity versus time

wave. First, we note that the state of uniform motion with a constant distance to the wall is easily destroyed under the influence of a potential wave. As a result, the distance to the wall changes, and the longitudinal and transverse components of the vortex velocity also change. In the moving coordinate frame, even of the vortex motion direction can change to the opposite one. Taking into account that a point vortex in the real fluid corresponds to the extensive linear vortex, we can expect the creation of the horseshoe-shaped and more complicated structures as a result of the interaction of a linear vortex with the inhomogeneous wave packets of sound waves.

Let us discuss how the small corrections arisen due to the vortex-induced potential waves influence the vortex motion. Based on the general properties of dynamical systems, we can expect that these corrections should lead to the destruction of separatrices and to the creation of narrow stochastic layers in their neighborhood. This means, in turn, the possibility of the vortex walk in the overlapping stochastic layers. In the rest of the phase space, the qualitative pattern of the vortex behavior should not dramatically change.

It should be noted that the modes causing the loss of the memory of the initial vortex position lead to a change in the energy of the vortical component. In an indirect way, this means that, in the wave—vortex system, we can observe the phenomenon similar to the collisionless decay of waves in plasma. In other words, the interaction of a potential wave with point vortices in the ideal fluid can lead to the change in the wave amplitude. However, the analysis of such phenomena requires a self consistent description of the interaction of waves and vortices within a quasilinear theory, and this analysis lies beyond the scope of the present paper.

1. H. Helmholtz, J. rein, angew. Math. **55**, 25—55 (1858).
2. G. Kirchhoff, *Mechanics. Lectures on Mathematical Physics* (AS USSR, Moscow, 1962) (in Russian).
3. V.V. Melehsko, M.Yu. Konstantinov, *Dynamics of the Vortical Structures* (Naukova Dumka, Kyiv, 1993) (in Russian).
4. W. Gröbli, Vierteljahrsch. d. Naturforsch. Geselsch. **22**, 37—81 (1877).
5. J.L. Synge, Can. J. Math. **1**, 257—270 (1949).
6. E.A. Novikov, Zh. Eksp. Teor. Fiz. **68**, N5, 1868—1882 (1975).
7. H. Aref, Phys. Fluids. **31**, N 6, 1392—1409 (1988).
8. S.L. Ziglin, Dokl. Akad. Nauk SSSR. **250**, N6, 1296—1300 (1979).
9. M.S.A.C. Castilla, V. Moauro, P. Negrini, W.M. Oliva, Ann. Inst. Henri Poincare: Phys. Theor. **59**, 1, 99—115 (1993).
10. J. Koiller, S.P. Carvalho, Commun. Math. Phys. **120(4)**, 643—652 (1989).
11. S.L. Ziglin, Physica D. **4**, 261—269 (1982).
12. E.J. Routh, Proc. Lond. Math. Soc. **12**, N 170/171, 73—89 (1991).
13. P.K. Newton, *The N-Vortex Problem: Analytical Techniques* (Springer, New York, 2001).
14. M.J. Lighthill, Proc. Roy. Soc. A. **211**, N 1107, 564—587 (1952).
15. M.J. Lighthill, Proc. Roy. Soc. A. **222**, N1148, 1—32 (1954).
16. V.Yu. Gonchar, P.N. Ostapchuk, A.V. Tur, V.V. Yanovsky, Phys. Lett. A. **152**, N 5/6, 287—292 (1991).
17. Yu.L. Bolotin, A.V. Tur, V.V. Yanovsky, *Constructive Chaos* (Institute for Single Crystals, Kharkiv, 2005) (in Russian).
18. L.D. Landau, E.M. Lifshits, *Fluid Dynamics* (Nauka, Moscow, 1986) (in Russian).
19. G. Helmholtz, *Two Investigations in Fluid Dynamics* (Nauka, Moscow, 1902), P.5—51 (in Russian).
20. N.N. Bautin, E.A. Leontovich, *Methods and Techniques of the Qualitative Study of Dynamical Systems in Plane* (Nauka, Moscow, 1990) (in Russian)).
21. V.I. Arnold, *Mathematical Methods of Classical Mechanics* (Nauka, Moscow, 1989) (in Russian).

Received 03.01.06.
Translated from Russian by M.L. Shendeleva

ЕВОЛЮЦІЯ ВИХОРУ ПОБЛИЗУ ТВЕРДОЇ СТІНКИ ПІД ВПЛИВОМ ПОТЕНЦІАЛЬНОЇ ХВИЛІ

К.М. Кулик, А.В. Тур, В.В. Яновський

Р е з ю м е

Вивчено дію потенціальних мод коливань на рух точкового вихору поблизу твердої стінки. Отримано рівняння, які описують рух точкового вихору у заданому полі потенціальної хвилі за наявності твердої стінки. Показано, що характер руху вихору під дією потенціальної хвилі змінюється. Проаналізовано всі можливі режими руху вихору під дією потенціальної хвилі.